Supplement of Biogeosciences, 18, 2405–2428, 2021
https://doi.org/10.5194/bg-18-2405-2021-supplement

Biogeosciences Open Access EGU

Supplement of

Plant phenology evaluation of CRESCENDO land surface models – Part 1: Start and end of the growing season

Daniele Peano et al.

Correspondence to: Daniele Peano (daniele.peano@cmcc.it)

This document contains:

- Supplementary Figure 1 contains the distribution of the four growing season types for the three satellite products;
- Supplementary Figure 2 contains the distribution of the agreement regions for the four growing season types between Land Surface Models (LSM) and LAI3g;
- Supplementary Table 1 contains the percentage of agreement for each growing season type between LAI3g and LSM;
- Supplementary Figure 3 contains the distribution of the agreement regions for the four growing season types between Land Surface Models (LSM) and CGLS;
- Supplementary Table 2 contains the percentage of agreement for each growing season type between CGLS and LSM;
- Supplementary Figure 4 contains the global climatological growing season start and end timings for LAI3g and CGLS;
- Supplementary Figure 5 contains the differences in growing season start timings between LAI3g and each Land Surface Model;
- Supplementary Figure 6 contains the differences in growing season end timings between LAI3g and each Land Surface Model;
- Supplementary Table 3 contains the fraction of land grid-cell in agreement with LAI3g for each land surface model in Onset and Offset timings;
- Supplementary Table 4 contains the average difference between LAI3g and MODIS, CGLS, each land surface model, and multi-model ensemble mean (MME) in Growing Season Start (GSS) and Growing Season End (GSE) timings;
- Supplementary Figure 7 contains the differences in growing season start timings between CGLS and each Land Surface Model;
- Supplementary Figure 8 contains the differences in growing season end timings between CGLS and each Land Surface Model;
- Supplementary Table 5 contains the fraction of land grid-cell in agreement with CGLS for each land surface model in Onset and Offset timings;
- Supplementary Table 6 contains the average difference between CGLS and LAI3g, MODIS, each land surface model, and multi-model ensemble mean (MME) in Growing Season Start (GSS) and Growing Season End (GSE) timings;
- Supplementary Figure 9 contains the zonal mean of growing season start and end timings in three specific subregions: Americas; Europe plus Africa; Asia plus Oceania;
- Supplementary Figure 10 contains the distribution of the four growing season types of each Land Surface Model (LSMs) and MODIS.

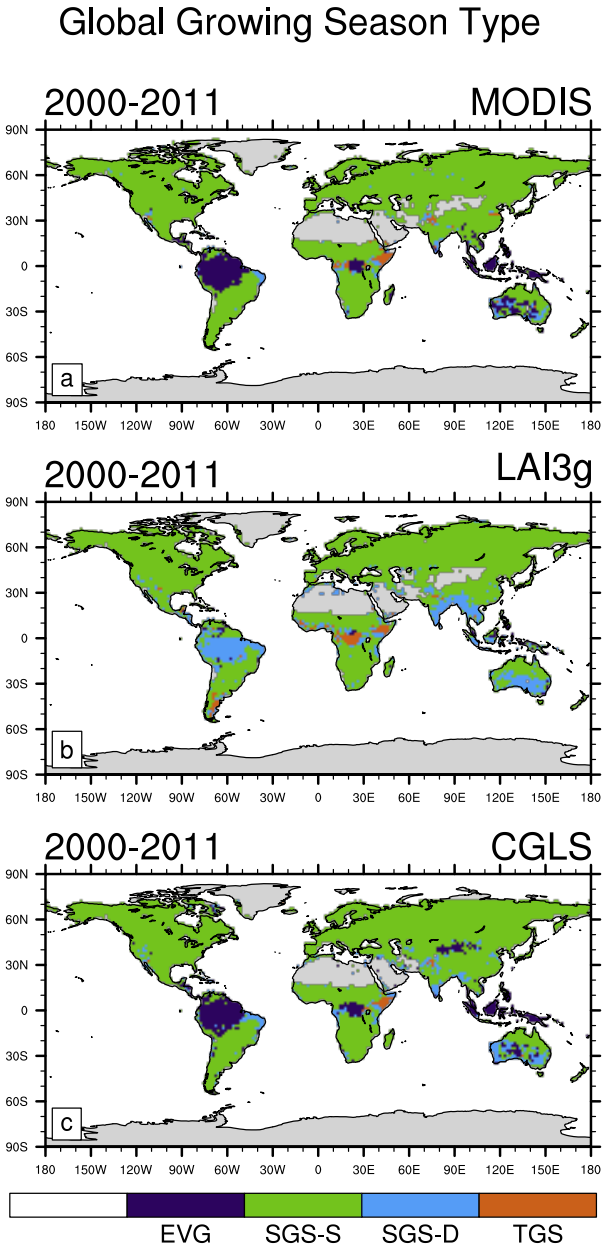

Supplementary Figure 1. Global climatological (averaged over 2000-2011) distribution of the four main growing season modes for (a) MODIS version 6, (b) LAI3g, (c) CGLS. Index values: (purple) evergreen; (green) single season with summer LAI peak; (cyan) single growing season with summer dormancy; (orange) two growing seasons type.

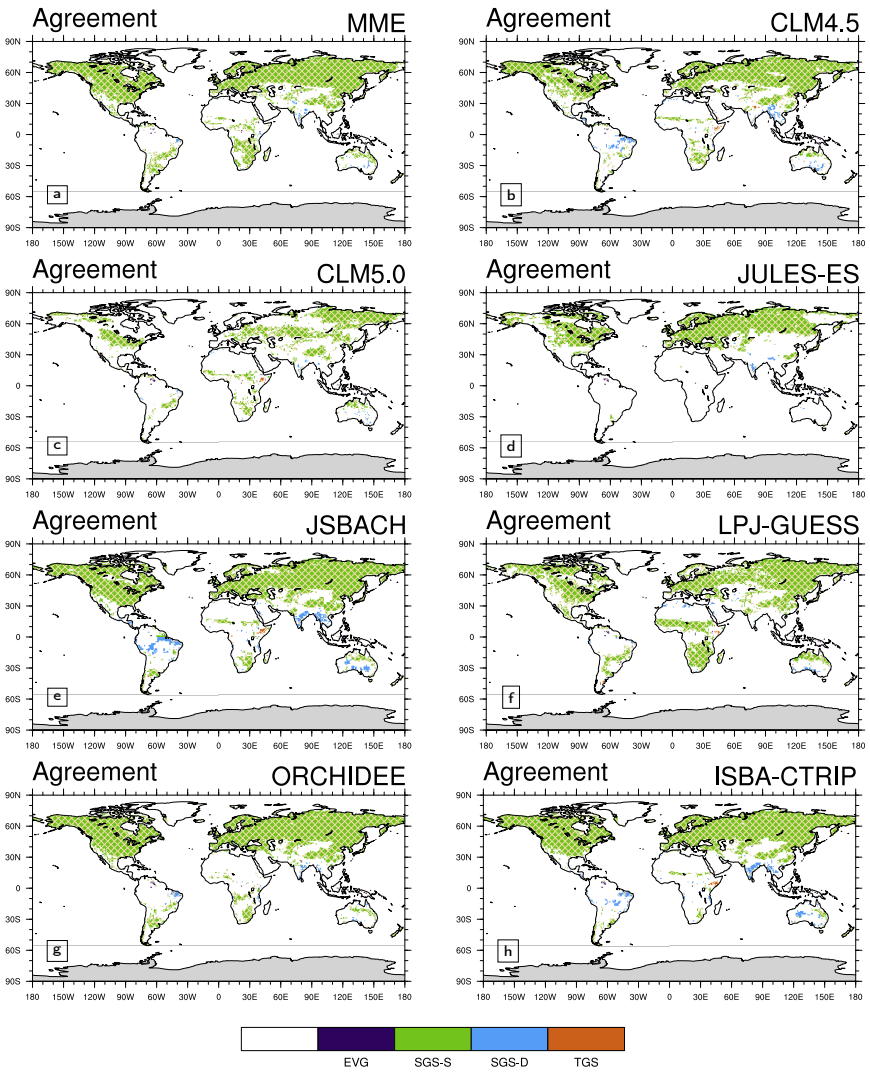

Supplementary Figure 2. Global climatological (averaged over 2000-2011) distribution of the four main growing season modes for (a) Multi-Model Ensemble mean (MME); (b) CLM 4.5; (c) CLM 5.0; (d) JULES-ES; (e) JSBACH; (f) LPJ-GUESS; (g) ORCHIDEE; (h) ISBA-CTRIP. Only the areas characterized by the same type of LAI3g (Supplemetary Figure 1b) are shown. These common areas are called agreement regions. Index values: (purple) evergreen; (green) single season with summer LAI peak; (cyan) single growing season with summer dormancy; (4, orange) two growing seasons type. White regions are for disagreement areas. Above this selection, areas of agreement between satellite products are shaded with a different hatching pattern: LAI3g and MODIS (Supplementary Figure 1a) slash hatching (/); LAI3g and CGLS (Supplementary Figure 1c) backslash hatching (\); MODIS, CGLS, and LAI3g crossed hatching (X).

Supplementary Table 1. Fraction of land grid-cell in agreement with LAI3g for Multi-Model Ensemble mean (MME) and LSMs in each growing season type. Values are reported in percentage. Colored regions in Supplementary Figure 2.

	CLM 4.5	CLM 5.0	JULES-ES	JSBACH	LPJ-GUESS	ORCHIDEE	ISBA-CTRIP	MME
EVG	56.4	73.7	90.1	21.8	61.2	71.1	72.0	40.2
SGS-S	67.4	44.0	50.4	75.3	76.0	81.3	77.0	78.9
SGS-D	37.4	20.8	5.0	41.1	17.9	20.6	39.6	13.1
TGS	14.0	9.8	0.3	8.3	14.1	3.8	7.1	0.5
Total	58.9	40.3	40.3	64.7	62.4	66.3	66.2	62.6

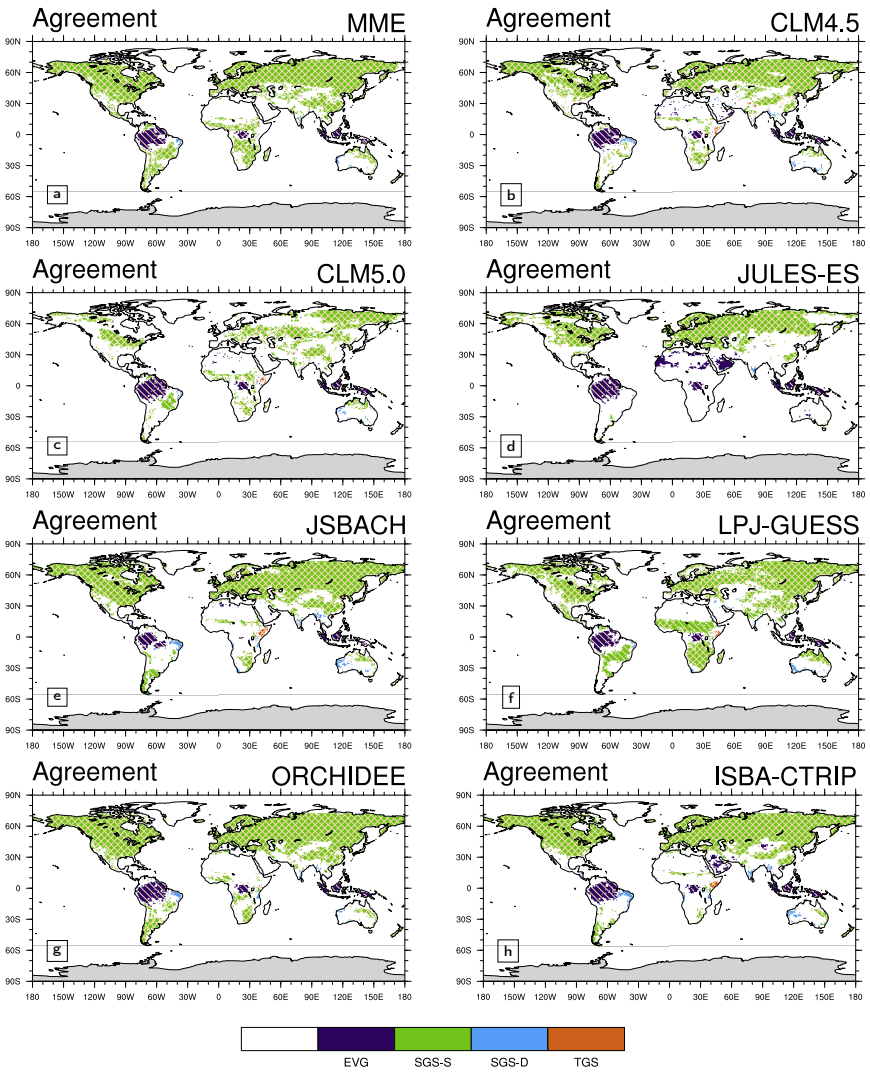

Supplementary Figure 3. Global climatological (averaged over 2000-2011) distribution of the four main growing season modes for (a) Multi-Model Ensemble mean (MME); (b) CLM 4.5; (c) CLM 5.0; (d) JULES-ES; (e) JSBACH; (f) LPJ-GUESS; (g) ORCHIDEE; (h) ISBA-CTRIP. Only the areas characterized by the same type of CGLS (Supplemetary Figure 1c) are shown. These common areas are called agreement regions. Index values: (1, purple) evergreen; (2, green) single season with summer LAI peak; (3, cyan) single growing season with summer dormancy; (4, orange) two growing seasons type. White regions are for disagreement areas. Above this selection, areas of agreement between satellite products are shaded with a different hatching pattern: LAI3g and CGLS (Supplementary Figure 1b) slash hatching (/); MODIS and CGLS (Supplementary Figure 1a) backslash hatching (\); MODIS, CGLS, and LAI3g crossed hatching (X).

Supplementary Table 2. Fraction of land grid-cell in agreement with CGLS for Multi-Model Ensemble mean (MME) and LSMs in each growing season type. Values are reported in percentage. Colored regions in Supplementary Figure 3.

	CLM 4.5	CLM 5.0	JULES-ES	JSBACH	LPJ-GUESS	ORCHIDEE	ISBA-CTRIP	MME
EVG	41.3	46.2	75.4	22.5	32.8	39.2	57.9	29.5
SGS-S	65.3	44.8	48.1	73.0	75.1	79.3	74.1	79.2
SGS-D	42.4	26.5	5.6	43.9	28.8	26.2	47.7	16.6
TGS	21.6	17.8	0.6	14.0	17.8	6.4	13.6	0.7
Total	58.3	42.4	46.5	61.0	63.0	66.3	67.2	63.8

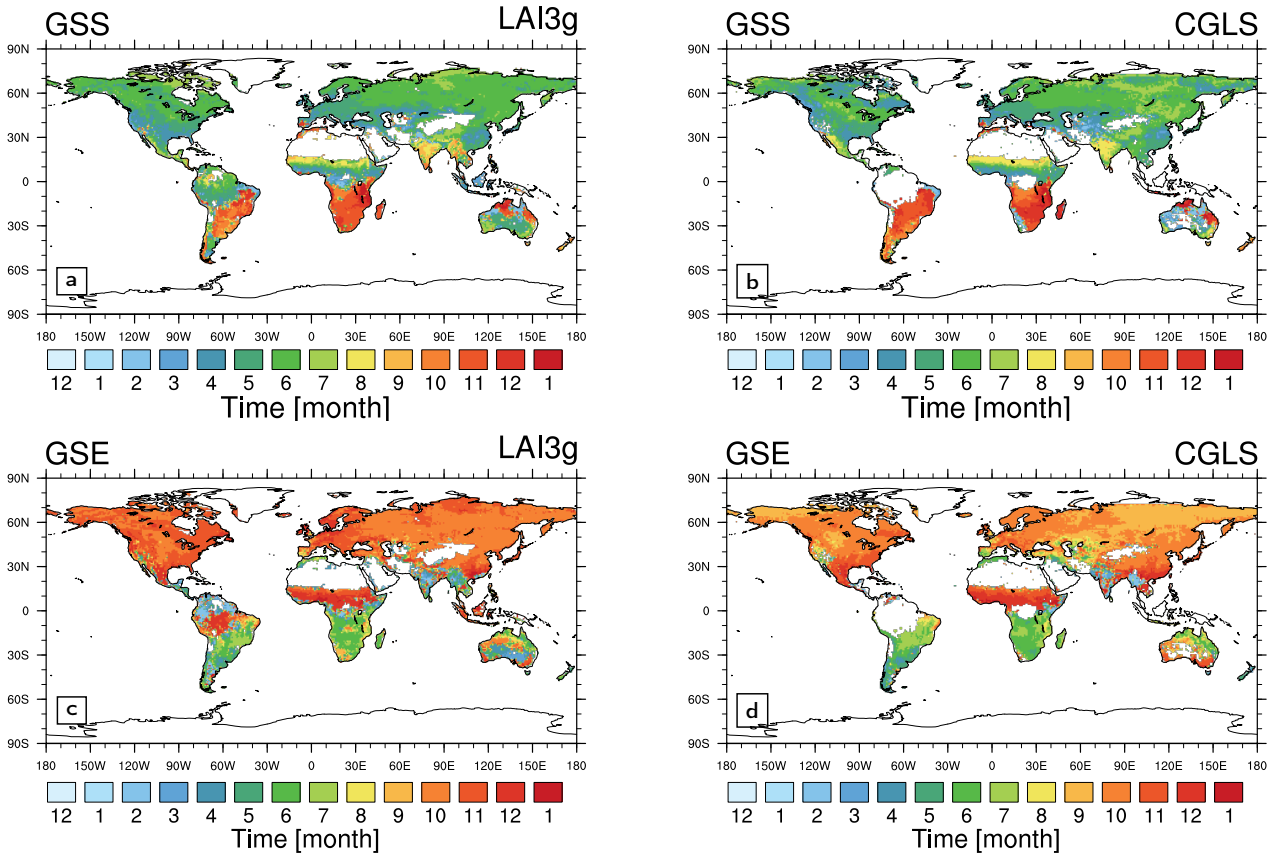

Supplementary Figure 4. Global climatological (averaged over 2000-2011) growing season (a,b) start (GSS) and (c,d) end (GSE) timings for (a,c) LAI3g, and (b,d) CGLS.

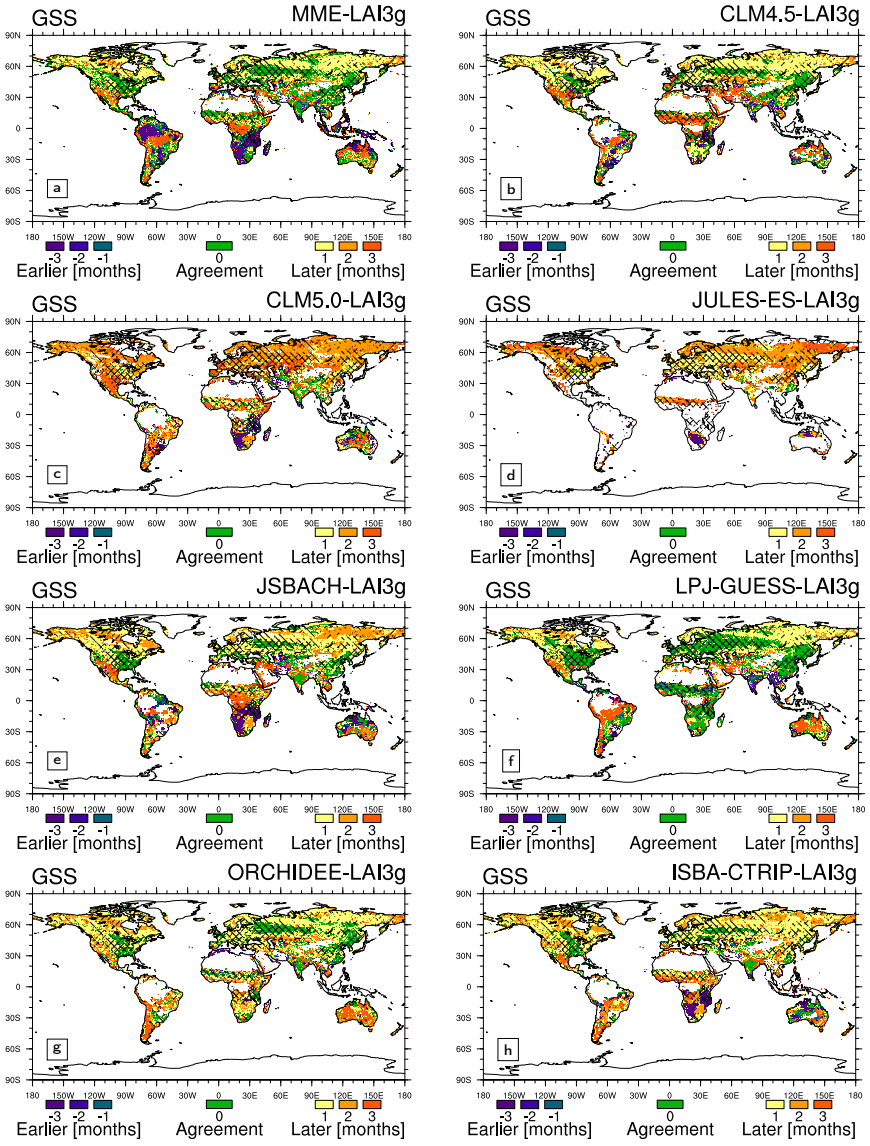

Supplementary Figure 5. Global climatological (averaged over 2000-2011) differences in growing season start (GSS) between (a) Multi-Model Ensemble mean (MME); (b) CLM 4.5; (c) CLM 5.0; (d) JULES-ES; (e) JSBACH; (f) LPJ-GUESS; (g) ORCHIDEE; (h) ISBA-CTRIP and LAI3g (Supplementary Figure 4a). The green regions represent areas of agreement between LAI3g and LSMs. Yellow-red colors correspond to areas where models timings are later compared to LAI3g, while blue-violet colors correspond to areas where models timings are earlier compared to LAI3g. Regions where GSS timings are not computed, such as non-vegetated and evergreen areas, are in white. Above this selection, areas of agreement between satellite products are shaded with a different hatching pattern: LAI3g and MODIS (Supplementary Figure 1a) slash hatching (/); LAI3g and CGLS (Supplementary Figure 1c) backslash hatching (\); MODIS, CGLS, and LAI3g crossed hatching (X). Note that the GSS in the TGS regions corresponds to the GSS of the first growing season cycle

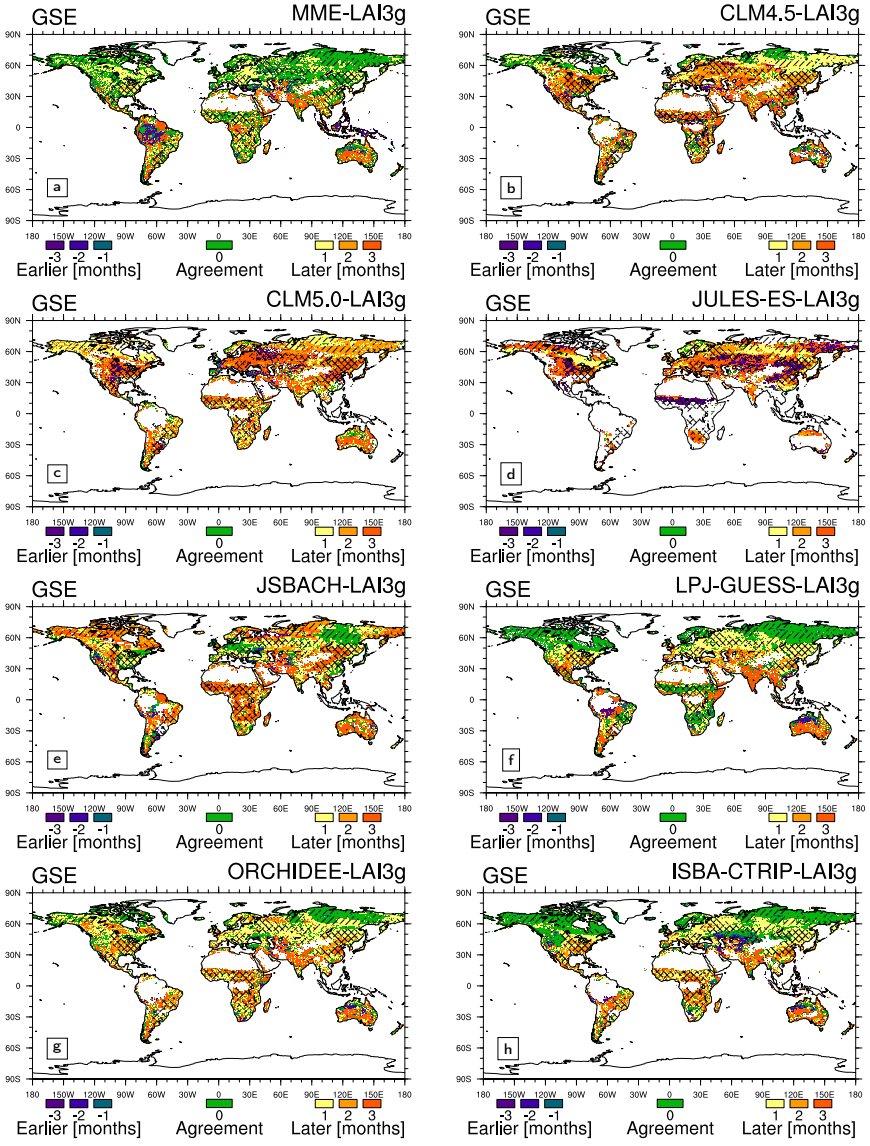

Supplementary Figure 6. As Supplementary Figure 5 but for growing season end (GSE) timings between LAI3g (Supplementary Figure 4c) and Multi-Model Ensemble mean (MME) and LSMs. Note that the GSE in the TGS regions corresponds to the GSE of the second growing season cycle.

Supplementary Table 3. The fraction of land grid-cell in agreement with LAI3g for MODIS, CGLS, each land surface model, and multi-model ensemble mean (MME) in growing season start (GSS) and growing season end (GSE) timings. Values are reported in percentages for global, North Hemisphere (NH), and South Hemisphere (SH). Green shaded areas in Supplementary Figures 5 and 6. The last row reports the fraction of land grid-cell in agreement with MODIS for each land surface model in growing season length. The values in brackets give the percentage of global, NH, and SH with a maximum difference of one month.

	MODIS	CGLS	CLM 4.5	CLM 5.0	JULES-ES	JSBACH	LPJ-GUESS	ORCHIDEE	ISBA-CTRIP	MME
GSS	34.3	39.4	17.1	5.7	1.9	15.7	25.6	21.7	13.6	16.1
	(66.9)	(71.3)	(52.0)	(20.8)	(16.7)	(50.3)	(57.1)	(58.4)	(55.7)	(38.3)
GSE	40.9	28.7	16.4	5.0	2.3	13.7	22.5	21.6	22.4	23.3
	(72.5)	(66.3)	(38.8)	(22.8)	(11.7)	(36.1)	(54.7)	(54.6)	(58.6)	(43.0)
GSS NH	37.0	43.1	19.0	5.4	2.4	17.9	27.9	24.8	15.5	17.7
	(72.2)	(77.1)	(59.1)	(21.6)	(20.9)	(58.8)	(62.3)	(66.3)	(65.5)	(43.0)
GSE NH	44.8	29.4	17.9	4.2	2.8	15.4	24.8	25.1	26.1	26.3
	(79.2)	(70.8)	(42.1)	(22.5)	(14.6)	(39.9)	(60.3)	(62.0)	(67.0)	(47.7)
GSS SH	24.9	26.5	10.5	6.8	0.4	8.1	18.0	11.2	7.1	10.7
	(48.7)	(51.4)	(27.3)	(18.0)	(2.1)	(20.8)	(39.3)	(31.2)	(21.9)	(22.0)
GSE SH	27.4	26.4	11.4	7.7	0.5	7.8	14.8	9.3	9.7	13.0
	(49.5)	(50.7)	(27.4)	(23.7)	(1.6)	(23.0)	(35.7)	(28.8)	(29.5)	(26.7)
Length	24.6	22.2	16.2	17.2	12.7	16.3	13.5	19.4	18.2	26.1
	(55.8)	(55.8)	(42.6)	(43.5)	(34.1)	(49.4)	(44.6)	(53.0)	(47.0)	(52.3)

Supplementary Table 4. Average difference between LAI3g and MODIS, CGLS, each land surface model, and multi-model ensemble mean (MME) in Growing Season Start (GSS) and Growing Season End (GSE) timings. Values are reported in months for global, North Hemisphere (NH) and South Hemisphere (SH). Positive values stand for later timings and negative values correspond to earlier timings.

	MODIS	CGLS	CLM 4.5	CLM 5.0	JULES-ES	JSBACH	LPJ-GUESS	ORCHIDEE	ISBA-CTRIP	MME
GSS	-0.25	0.04	0.31	0.54	0.84	0.09	0.22	0.42	0.15	0.33
GSE	0.16	-0.09	-0.08	-0.86	-2.09	-0.03	0.35	0.07	-0.13	-0.27
GSS NH	-0.41	-0.04	0.55	1.07	1.03	0.55	0.06	0.29	0.54	0.54
GSE NH	0.31	-0.13	-0.09	-1.29	-2.36	-0.32	0.47	-0.02	-0.30	-0.45
GSS SH	0.42	0.38	-0.67	-1.73	-2.20	-1.81	0.81	0.97	-1.52	-0.49
GSE SH	-0.46	0.06	-0.07	0.97	2.35	1.16	-0.10	0.44	0.56	0.44

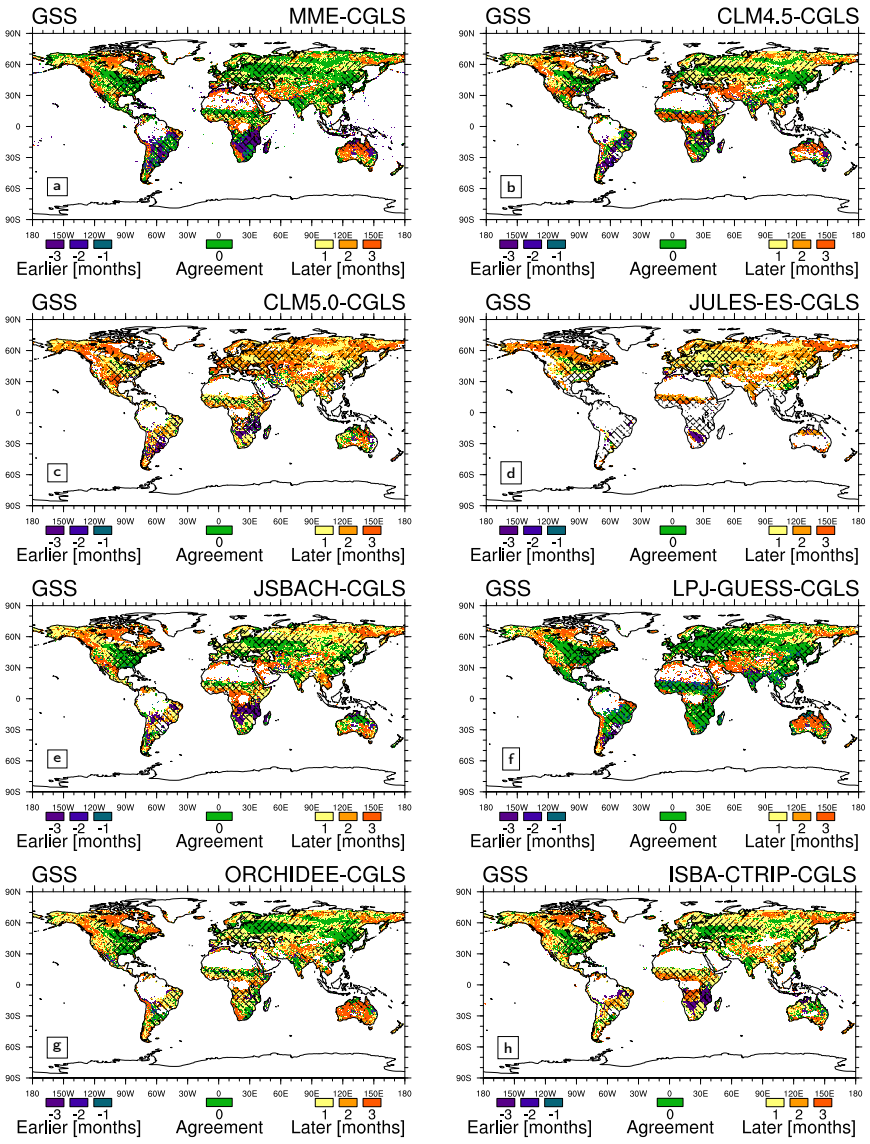

Supplementary Figure 7. As Supplementary Figure 5 but for growing season start (GSS) timings between CGLS (Supplementary Figure 4b) and Multi-Model Ensemble mean (MME) and LSMs. Note that areas of agreement between satellite products are shaded with a different hatching pattern: LAI3g and CGLS (Supplementary Figure 1b) slash hatching (/); MODIS and CGLS (Supplementary Figure 1a) backslash hatching (\); MODIS, CGLS, and LAI3g crossed hatching (X).

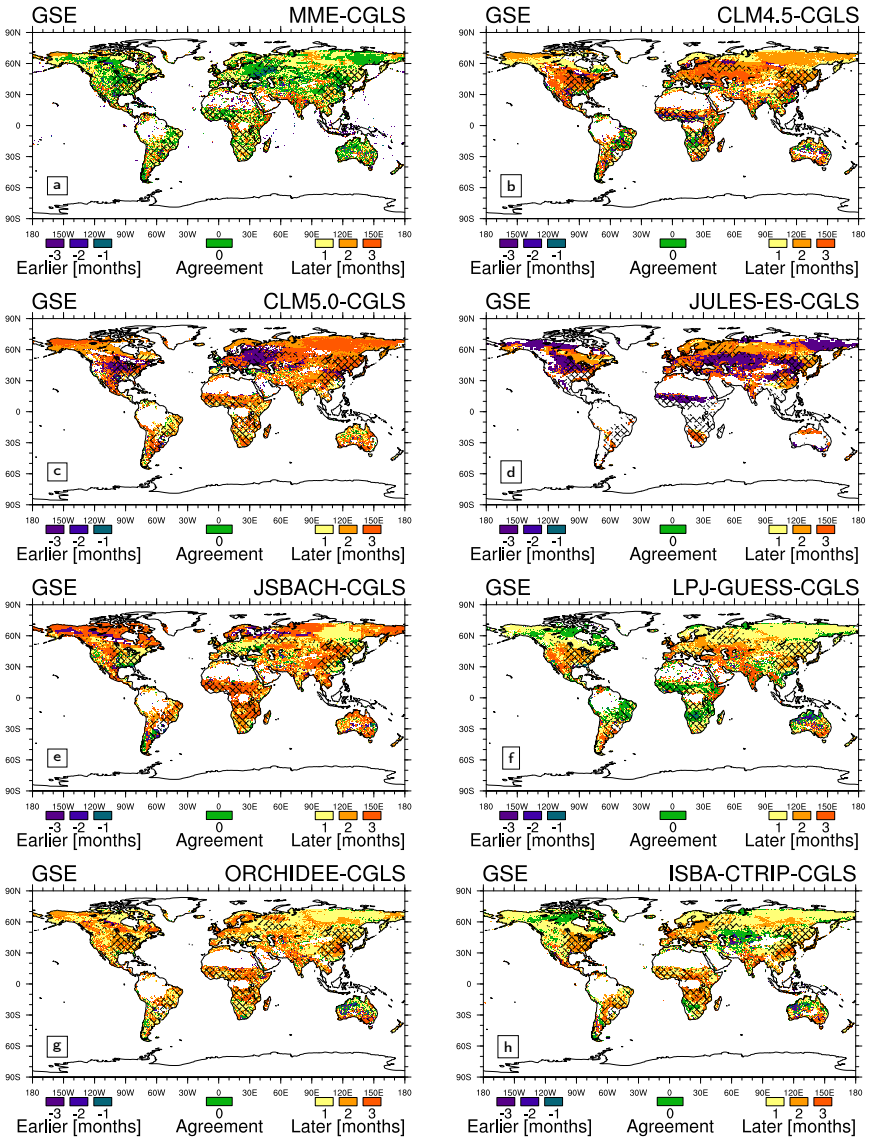

Supplementary Figure 8. As Supplementary Figure 6 but for growing season end (GSE) timings between CGLS (Supplementary Figure 4d) and Multi-Model Ensemble mean (MME) and LSMs.

Supplementary Table 5. The fraction of land grid-cell in agreement with CGLS for MODIS, LAI3g, each land surface model, and multi-model ensemble mean (MME) in growing season start (GSS) and growing season end (GSE) timings. Values are reported in percentages for global, North Hemisphere (NH), and South Hemisphere (SH). Green shaded areas in Supplementary Figures 7 and 8. The last row reports the fraction of land grid-cell in agreement with MODIS for each land surface model in growing season length. The values in brackets give the percentage of global, NH, and SH with a maximum difference of one month.

	LAI3g	MODIS	CLM 4.5	CLM 5.0	JULES-ES	JSBACH	LPJ-GUESS	ORCHIDEE	ISBA-CTRIP	MME
GSS	42.1	42.2	24.3	7.3	3.2	24.3	28.1	29.5	24.1.	26.0
	(76.2)	(71.6)	(53.0)	(32.1)	(25.8)	(57.2)	(57.5)	(60.5)	(62.2)	(49.6)
GSE	30.3	32.4	7.5	3.2	0.1	5.9	18.2	7.6	16.8.	19.7
	(69.9)	(67.3)	(27.8)	(11.8)	(2.6)	(28.6)	(55.4)	(42.7)	(56.8)	(39.5)
GSS NH	44.4	38.6	26.9	6.7	3.9	26.8	31.3	32.4	26.6	29.3
	(79.4)	(70.6)	(58.1)	(33.1)	(31.3)	(62.9)	(60.3)	(65.3)	(68.2)	(55.9)
GSE NH	29.8	28.5	5.3	2.2	0.1	5.7	17.0	6.6	17.5	20.0
	(72.0)	(65.5)	(26.0)	(7.8)	(2.9)	(30.3)	(54.9)	(44.2)	(60.8)	(39.9)
GSS SH	32.5	56.7	14.1	9.9	0.6	13.9	14.7	17.5	13.7	12.4
	(62.9)	(75.7)	(32.0)	(28.1)	(3.2)	(33.9)	(45.9)	(41.2)	(37.4)	(23.7)
GSE SH	32.0	48.7	16.3	7.3	0.1	6.4	22.9	11.6	13.6	18.5
	(61.4)	(74.8)	(35.5)	(28.0)	(1.2)	(21.6)	(57.2)	(36.8)	(40.4)	(37.6)
Length	23.1	27.7	10.2	13.1	13.4	16.5	12.5	16.0	24.2	22.2
	(58.1)	(52.0)	(32.0)	(38.9)	(36.1)	(45.4)	(42.5)	(49.3)	(56.2)	(46.0)

Supplementary Table 6. Average difference between CGLS and LAI3g, MODIS, each land surface model, and multi-model ensemble mean (MME) in Growing Season Start (GSS) and Growing Season End (GSE) timings. Values are reported in month for global, North Hemisphere (NH) and South Hemisphere (SH). Positive values stand for later timings and negative values correspond to earlier timings.

	LAI3g	MODIS	CLM 4.5	CLM 5.0	JULES-ES	JSBACH	LPJ-GUESS	ORCHIDEE	ISBA-CTRIP	MME
GSS	-0.04	-0.30	0.23	0.52	0.79	0.07	0.13	0.35	0.11	0.27
GSE	0.09	0.31	0.03	-0.79	-1.77	0.06	0.44	0.22	0.02	-0.19
GSS NH	0.04	-0.38	0.59	1.09	0.96	0.58	0.09	0.30	0.58	0.60
GSE NH	0.13	0.48	0.05	-1.16	-2.05	-0.16	0.59	0.20	-0.10	-0.35
GSS SH	-0.38	0.01	-1.30	-2.01	-2.06	-2.30	0.31	0.59	-1.97	-1.12
GSE SH	-0.06	-0.39	-0.06	0.84	2.77	1.11	-0.18	0.34	0.56	0.46

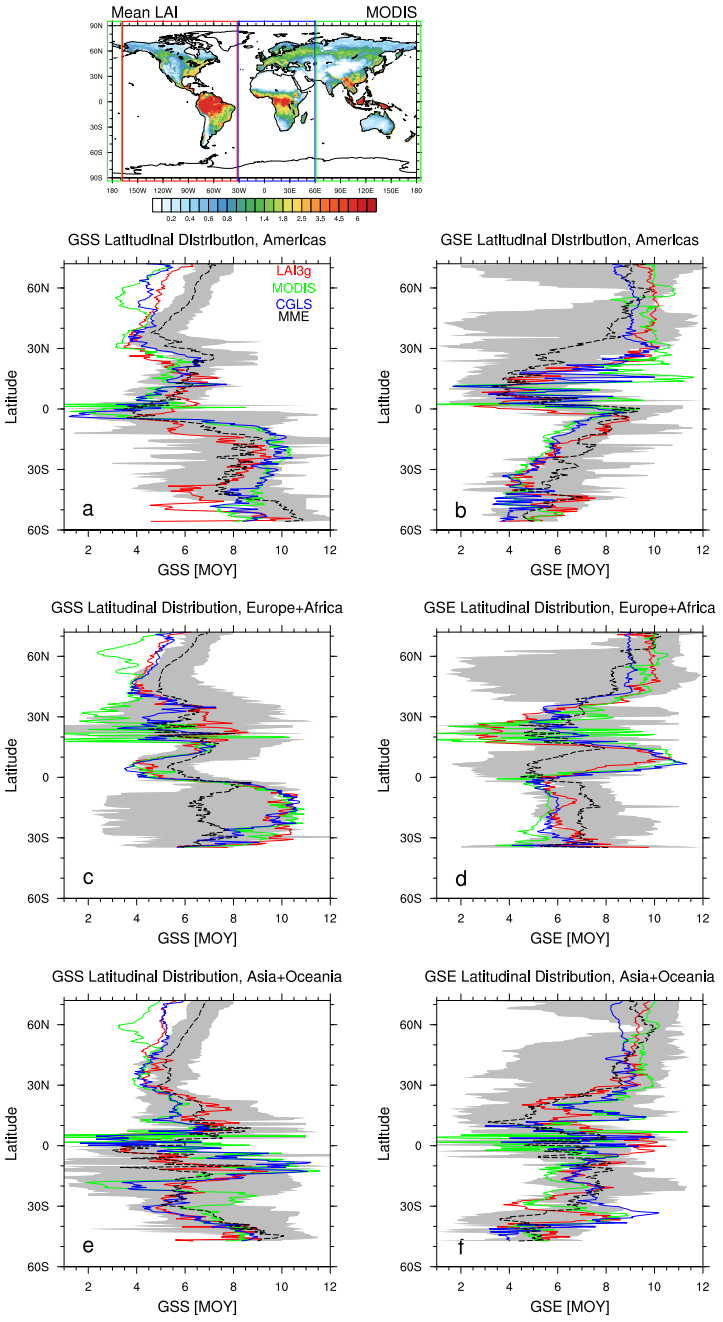

Supplementary Figure 9. Zonal mean (a,c,e) growing season start (GSS) and (b,d,f) growing season end (GSE) timings for LAI3g (red lines), MODIS (green lines), CGLS (blue lines), and multi-model ensemble mean (black dashed line). The grey regions show the multi-model ensemble spread. The zonal means are computed over three specific regions: (a,b) Americas (170 – 35°W, red rectangle in the upper map); (c,d) Europe plus Africa (35°W – 60°E, blue rectangle in the upper map); (e,f) Asia plus Oceania (60°E – 170°W, green rectangle in the upper map). Values are reported as months of the year (MOY)

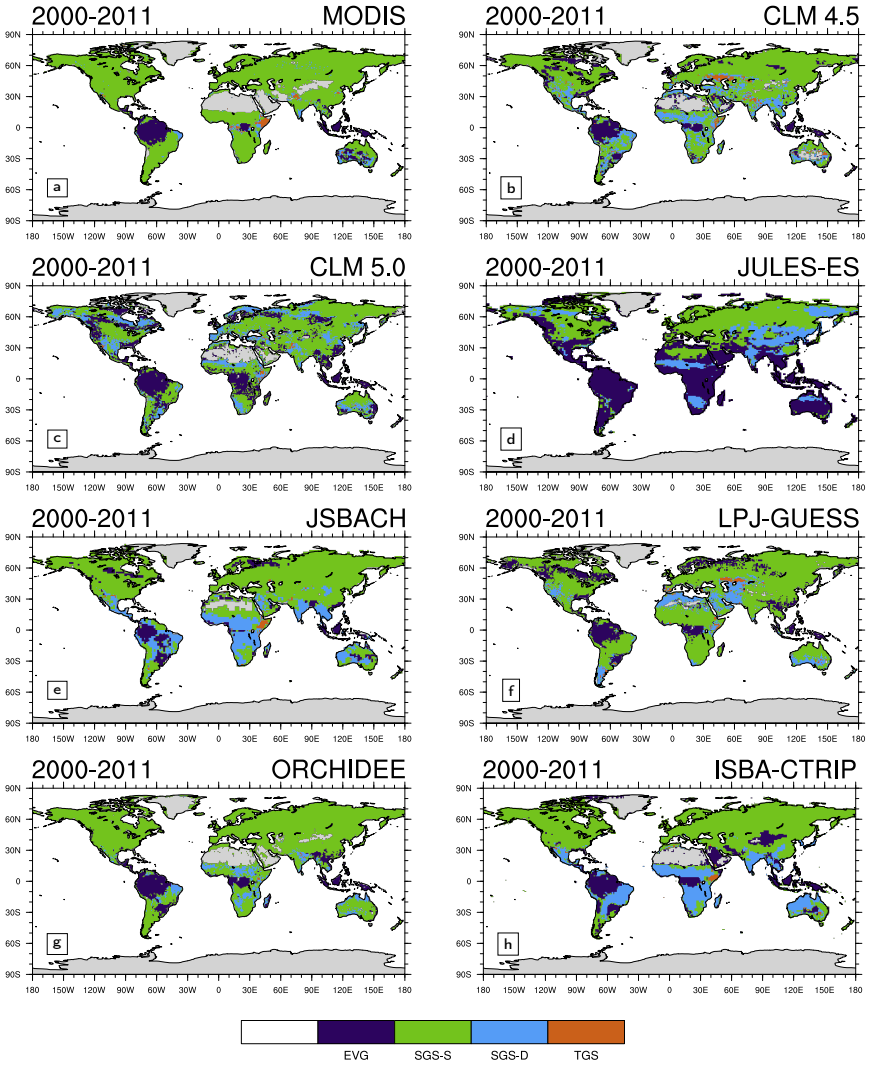

Supplementary Figure 10. Global climatological (averaged over 2000-2011) distribution of the four main growing season modes for (a) MODIS, (b) CLM 4.5; (c) CLM 5.0; (d) JULES-ES; (e) JSBACH; (f) LPJ-GUESS; (g) ORCHIDEE; (h) ISBA-CTRIP. Index values: (purple) evergreen; (green) single season with summer LAI peak; (cyan) single growing season with summer dormancy; (orange) two growing seasons type. It is important to keep in mind that evergreen regions are detected as areas where changes in annual LAI cycle are smaller than 25% of the local annual LAI mean value (*Peano et al.*, 2019).

References

Li, W., N. MacBean, P. Ciais, P. Defourny, C. Lamarche, S. Bontemps, R. A. Houghton, and S. Peng (2018), Gross and net land cover changes in the main plant functional types derived from the annual ESA CCI land cover maps (1992–2015), *Earth System Science Data*, *10*, 219–234, https://doi.org/10.5194/essd-10-219-2018

Peano, D., S. Materia, A. Collalti, A. Alessandri, A. Anav, A. Bombelli, and S. Gualdi (2019), Global variability of simulated and observed vegetation growing season, *JGR: Biogeosciences*, *124*, https://doi.org/10.1029/2018JG004881.